Electron collisions with the CN radical: bound states and resonances

2012 J. Phys. B: At. Mol. Opt. Phys. 45 035204

(http://iopscience.iop.org/0953-4075/45/3/035204)

J. Phys. B: At. Mol. Opt. Phys. **45** (2012) 035204 (7pp) doi:10.1088/0953-4075/45/3/035204

Electron collisions with the CN radical: bound states and resonances

Stephen Harrison and Jonathan Tennyson

Department of Physics and Astronomy, University College London, Gower St., London WC1E 6BT, UK

E-mail: stephen.harrison@ucl.ac.uk

Received 3 October 2011, in final form 22 December 2011
Published 16 January 2012
Online at stacks.iop.org/JPhysB/45/035204

Abstract

CN is a fundamental molecule found in numerous environments and as such it is important to understand the processes in which it can be involved in. Its counterpart anion, CN^-, was one of the first molecular anions to be detected in the interstellar medium (ISM). *Ab initio* electron–molecule scattering calculations for the neutral radical CN are presented. A number of target calculations are carried out to obtain a model which corresponds with experimental target data; these models test the use of different basis sets, and both Hartree–Fock and natural orbitals. A range of scattering models are considered, including static exchange and close-coupling methods. Results are presented for bound and resonance states of the anion, eigenphase sums, elastic cross-sections and electronic excitation cross-sections for electron scattering with the neutral radical. These results are subsequently analysed at a range of bond lengths. It is found that the electronic resonances are all too high in energy to be important for anion formation in the interstellar medium. Electron impact electronic excitation is considered to the $A\,^2\Pi$ and $B\,^2\Sigma^+$ states, source of the 'CN red' and 'CN violet' electronic bands respectively.

(Some figures may appear in colour only in the online journal)

1. Introduction

The CN radical is a well-known and a well-studied molecule, particularly through its spectra. A review of previous work on this can be found in the introduction of Liu *et al* (2001). CN is found in numerous environments, ranging from the sun's atmosphere to terrestrial plasmas and within flames (Halpern *et al* 1996). It was also one of the first molecules used to study the cosmic microwave background (Thaddeus 1972), and is still studied today (Leach 2012). Within these diverse but hostile environments CN can undergo a variety of processes. In this paper we concentrate on electron collisions with the radical CN.

Information on electron scattering is important as such collisions may cause electronic excitations. This produces the electronic emission spectra crucial in identifying the molecule in a range of environments. Modelling these spectra requires knowledge of appropriate electronic excitation mechanisms. Here we consider the interactions between the target radical and the scattering electron and, in particular, the first two excitations of molecular CN, the $X^2\Sigma^+$–$A^2\Pi$ and $X^2\Sigma^+$–$B^2\Sigma^+$ transitions. These give rise to the 'CN red' and 'CN violet' spectral bands.

The anionic form, CN^-, is also the smallest molecular anion to be have been observed in space (Agundez *et al* 2010). This detection used observations of the $J = 2 - 1$ and $J = 3 - 2$ rotational transitions in the envelope of carbon star IRC +10216; these transitions were recently measured experimentally in the laboratory by Gottlieb *et al* (2007). Here CN^- was found in high abundance: 0.25%, relative to neutral CN, in comparison to the extremely small abundance of C_2H^- relative to its neutral in the same region. The reason for the relative sparseness of C_2H^- in comparison to other observed small linear carbon chains has previously been discussed in Harrison and Tennyson (2011). As the rate of formation of the anion due to radiative electron attachment is very slow for the smallest carbon chains, such as CN^-, here we investigate the possibility that the formation rate is enhanced by very weakly bound anion states. This mechanism has been proposed for the linear, carbon-chain anions recently detected in space (Herbst and Osamura 2008, Harrison and Tennyson 2011).

Surprisingly, given its importance, there is very little previous work on electron collisions with CN. Experimental

electron collision studies are common for stable diatomics (Brunger and Buckman 2002) but difficult for radicals and we are unaware of any for CN. Many theoretical methods are not constrained by the need for a stable target structure, including the one we present below. However the only calculated e^--CN collision cross-sections are due to Joshipura and Patel (1994), who considered total cross-sections at high energies (100–1000 eV). Our work therefore represents the first study of low-energy electron collision behaviour with the CN radical.

2. Method

Scattering calculations were performed using the *R*-matrix method (Burke 2011), whose use for collision calculations involving molecules has recently been extensively reviewed by one of us (Tennyson 2010). The basic idea of the *R*-matrix method is the division of space into two regions: a spherical inner region of radius a which is designed to enclose all the charge density of the target, and an outer region where interactions between the electron and the target can be represented by long-range moments. The major advantage of the method is that within the inner region the problem is solved independent of the energy of the scattering electron. Within this region the wavefunction is written as

$$\psi_k^{N+1} = \mathcal{A} \sum_{ij} a_{ijk} \Phi_i^N(\mathbf{x}_1 \cdots \mathbf{x}_N) u_{ij}(\mathbf{x}_{N+1}) + \sum_i b_{ik} \chi_i^{N+1}(\mathbf{x}_1 \cdots \mathbf{x}_{N+1}), \quad (1)$$

where the target contains N electrons and functions are labelled as N or $N+1$ according to whether they refer to the target or the compound scattering system respectively. In this work we use the polyatomic *R*-matrix code (Morgan *et al* 1998) and all orbitals used to construct the wavefunctions of equation (1) were constructed from Gaussian-type orbitals. As discussed below a variety of different target orbital sets (Hartree–Fock (HF), CASSCF and natural orbitals (NOs)) were tested. In this regard one important issue is the requirement to represent all target states included in the calculation with a single orbital set.

In equation (1), Φ_i^N is the wavefunction of ith target state. u_{ij} are the extra orbitals introduced to represent the scattering electron (Faure *et al* 2002). The operator $\mathcal{A}$ ensures that the product of these two terms obeys the Pauli principle. The second summation in equation (1) involves L^2 configurations which have no amplitude on the *R*-matrix boundary and where all electrons are placed in orbitals associated with the target. As we are dealing with electron collision with strongly dipolar systems, it is necessary to allow for the contribution of electron interactions with the long-range target dipole moment to any cross-sections calculated. This was carried out using the program BORNCROS (Baluja *et al* 2000), which directly calculates the dipole Born correction to both the total cross-sections and the dipole allowed excitation cross-sections.

The scattering calculations reported here were performed using the UK molecular *R*-matrix codes (Morgan *et al* 1998). In order to simplify the calculation, the Quantemol-N interface (Tennyson *et al* 2007) has been used for models 1–4 (see the target calculations section for details on these models). This software acts as an expert system to the *R*-matrix procedure, automatically generating the correct calculation inputs for the *R*-matrix codes using some simple parameters such as molecular geometry and basis set. In addition to using the Quantemol-N software, calculations inputs were also created manually and used directly in the *R*-matrix codes. This was done in order to allow to use of molecular orbitals different from the standard HF orbitals which the *R*-matrix codes produce. To produce these non-standard orbitals the quantum chemistry software MOLPRO (Werner *et al* 2008) has been used to calculate and output NOs, via the multi-reference configuration interaction (MRCI) method.

Scattering calculations were performed at two levels: static exchange (SE), which is useful for identifying shape resonances and close coupling (CC). The presence of low-lying excited target states meant that the widely used one-state SE plus polarization model was deemed inappropriate for this study, as this method is prone to give pseudo-resonances at energies above the first electronically excited target state. Calculations were carried out with an *R*-matrix radius of 15 a_0, this was to ensure all of the more diffuse augmented basis set used are entirely enclosed within the *R*-matrix sphere.

All calculations were initially performed at the CN equilibrium geometry 1.1718 Å, and ignored effects due to nuclear motion.

We note that although CN is linear, neither the polyatomic *R*-matrix codes nor MOLPRO use $C_{\infty v}$ symmetry. All calculations were therefore performed using C_{2v} symmetry but identifying the results in $C_{\infty v}$ proved to be straightforward and these symmetry labels are largely used below.

3. Target calculations

A variety of models were tested at r_e when calculating results for the neutral CN target, a selection of these are shown in table 1. Models 1–4 were carried out using the *R*-matrix expert system Quantemol-N. These comprised of HF and complete active space configuration-interaction (CAS-CI) calculations. Two basis sets, cc-pVTZ and aug-cc-pVTZ, were also used for each method. For the CAS-CI calculations an orbital space of 7, 2, 2 (for symmetries a_1, b_1, b_2) has been used. Mapping to 7 σ and 2 π orbitals in $C_{\infty v}$. Eight electrons were frozen in the 1–4σ orbitals with five active electrons distributed amongst the 5–7σ and 1–2π. Model 5 used this CAS-CI model but the molecular orbitals used in the calculation were the NOs produced by MOLPRO. For this model the scattering calculations were performed using the *R*-matrix codes manually, to allow for use of these orbitals. The NOs were state averaged from three separate MRCI calculations, one for each of the $^2A_1$, $^2B_1$ and $^2B_2$, ($^2\Sigma^+$ and $^2\Pi$) states, using the MOLPRO 'MATROP' facility. The weighting chosen for each state in the average was (using the above order of states) 5:1:1. This weighting was chosen as the pure $^2\Sigma^+$ (1:0:0) MRCI orbitals gave a vertical excitation energy which is too high but reproduced the experimental dipole moment excellently, and the equally state averaged (1:1:1) orbitals made the dipole moment too high by 0.5 Debye, although

Table 1. Selected calculated target properties of CN. All results are for the equilibrium geometry of CN. The calculated absolute energies of the X $^2\Sigma^+$ ground state are given in Hartree while the vertical excitation energy to the low-lying electronic states is given in eV. μ is the ground state dipole moment, given in Debye. See text for details of models.

Model	Basis	Orbitals	Method	X $^2\Sigma^+$	μ	A $^2\Pi$	B $^2\Sigma^+$
1	cc-pVTZ	SCF	HF	−92.217	2.260		
2	cc-pVTZ	SCF	CAS-CI	−92.290	1.167	1.538	3.910
3	aug-cc-pVTZ	SCF	HF	−92.218	2.307		
4	aug-cc-pVTZ	SCF	CAS-CI	−92.221	2.230	2.142	7.023
5	aug-cc-pVTZ	NOs	CAS-CI	−92.381	1.612	1.515	3.491
Thogersen and Olsen (2004)	cc-pVDZ		FCI	−92.493			
Berente *et al* (2002)	DZP	ROHF	CCSD	−92.508			
Sordo (2001)	CBS limit		CCSDT	−92.606			
Ajitha and Hirao (2001)	ANO		RCCSD			1.106	
Shi *et al* (2011)	AV5Z		MRCI+Q+CV+RE			1.141	3.194
Kalcher (2002)	cc-pVQZ		CAS-ACPF		1.44	1.141	
Polak and Fiser (2002)	aug-cc-pVQZ		CASSCF-MRCI		1.44		
Thompson and Dalby (1968)			Experiment		1.45		
Huber and Herzberg (1997)			Experiment			1.151	3.197

this model reproduced the vertical excitation energy found in the literature excellently. Because of this it was deemed that a weighting be used which approximated both parameters to a good degree without sacrificing the quality of one to improve the other. Having excitation energies too high would cause a shift in the threshold of the subsequent excitation cross-sections produced. Also when the Born correction is applied to these excitation cross-sections, its magnitude depends fundamentally on the square of the dipole moment. Hence approximating both of these molecular properties to a good degree is important to obtain a target which will lead to accurate scattering observables being produced in the finished calculation.

There have been a number of previous *ab initio* studies on CN; table 1 compares our models with the best of these. As we only use a very limited correlation space, the other studies give lower absolute energies even for calculations which use the same target basis. Our dipole moment for our final model gives agreement within 10% against the calculation of Kalcher (2002) and the experimental values of Thompson and Dalby (1968) and Polak and Fiser (2002). Absolute values of the dipole moment have been given, and in all cases the direction points towards the nitrogen atom. Our predictions for the vertical energy of excitation for the low-lying state are systematically too high for all models based on HF orbitals. Use of NOs greatly improves this situation; with these orbitals our excitation energies are 0.6 and 3.5 eV closer to the experimental values than model 4, which used HF orbitals but the same basis set. The best theoretical results, from the recent paper of Shi *et al* (2011), benefit from having the Davidson correction applied as well as including relativistic effects and core-valence correlation into the calculations. Note that the experimental excitation energies, taken from Huber and Herzberg (1997), are corrected to change from adiabatic to vertical excitation energies. This raises the original adiabatic values by some 0.06 eV (A) and 0.001 eV (B) giving vertical excitation energies given in the table.

4. Scattering calculations

Our scattering calculations provide a number of scattering observables, including total elastic and excitation cross-sections, eigenphase sums and resonance data and detection of anionic bound states. Three classes of model were tested: SE based on a single target state and using HF orbitals (the SCF-SE method), and two CC models where 48 state calculations (with the target composing of doublet and quartet states and six states per symmetry) were performed in the inner region. Of the two CC models, one used HF orbitals (SCF-CC), and the other using the MRCI NOs produced in MOLPRO (NO-CC).

Outer region calculations were performed retaining those target states which lie below 10 eV for the CC calculations, the Quantemol-N default setting. This means 16 and only four states were kept for models 2 and 4 respectively, and 15 for model 5. The results reported below are insensitive to increasing these numbers.

4.1. Cross-sections

Figure 1 presents the total elastic cross-section of CN for electron scattering energies up to 10 eV, for all three models with the aug-cc-pVTZ basis set, SCF-SE, SCF-CC and NO-CC. For the final NO-CC model, a Born correction was applied due to the dipolar nature of the molecule, which acts to increase the cross-section at all energies.

Electron impact electronic excitation cross-sections are given by the many-state CC calculations. Figure 2 shows the cross-sections representing the excitation from the $^2\Sigma^+$ ground state of the neutral to the first two excited states, A $^2\Pi$ and B $^2\Sigma^+$. Here the Born correction is applied to both excitations as they are both dipole allowed transitions; for clarity we only give corrected results for our calculation based on the use of NOs. The Born correction is small near threshold but becomes significant at higher collision energies, presumably as higher partial waves become important. Both excitation cross-sections show resonance features. The biggest difference between models is caused by the shift in excitation

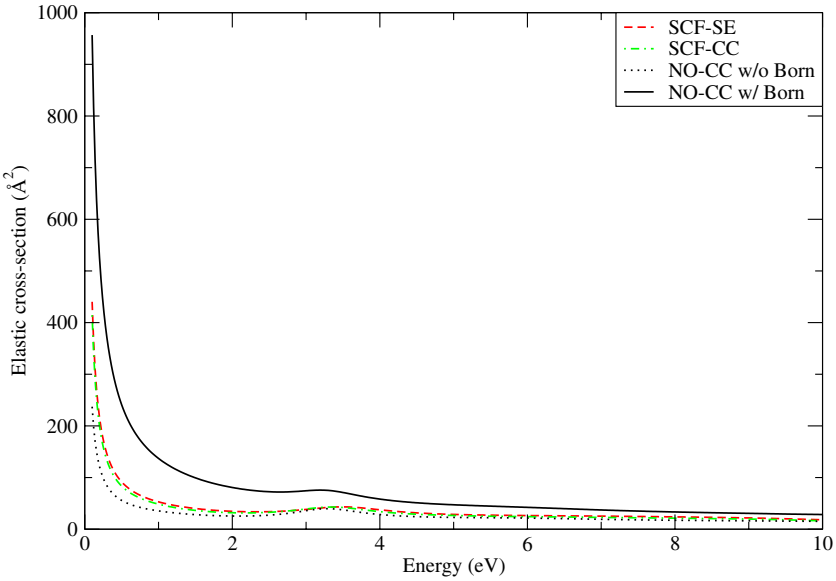

Figure 1. Elastic cross-section for electron CN collisions.

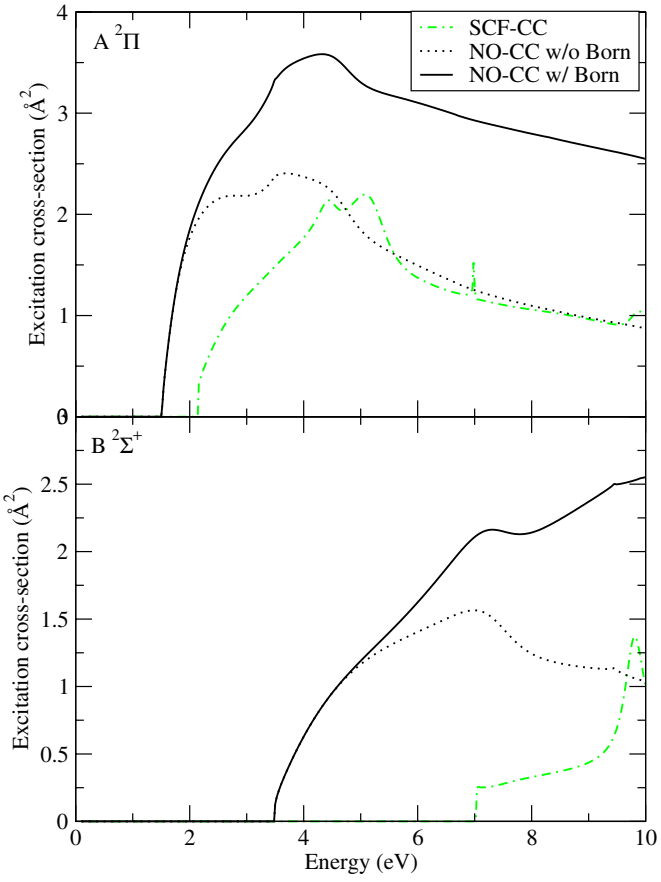

Figure 2. Electron impact electronic excitation cross-sections for CN final state: A $^2\Pi$, B $^2\Sigma^+$.

threshold. Since the NO-based calculation gives excitation energies which agree more closely with experiment than the SCF-based calculations, these must be regarded as our best estimate for the electronic excitation cross-section.

4.2. Bound anionic states

Bound state energies were calculated by searching at negative scattering energies using the outer region program BOUND (Sarpal *et al* 1991). For these calculations only the low-lying X $^2\Sigma^+$ and A $^2\Pi$ were retained in the outer region of the CC calculations, since experience has shown that strongly closed states can cause such outer region calculations to be numerically unstable. These were propagated to a distance of 30.1 a_0. Table 2 summarizes the results of these studies. All models found only a single bound state. The SE calculations give a vertical binding energy of about 2.6 eV whereas for the CC calculations this binding energy is increased to between 3.4 and 3.8 eV. This figure is in good agreement with the full configuration interaction electronic structure calculations of Thogersen and Olsen (2004).

The use of density functional theory (Midda and Das 2004) gives an energy of 4.04 eV, 0.6 eV higher than our value despite using the same basis set. The NO-CC binding energy of our final model is some 0.4 eV less than both the calculated SCF-CC and the measured values; however the measured binding energies quoted are adiabatic and will therefore be larger than our calculated vertical ones. The work of Polak and Fiser (2002) agrees within 5% of our best value despite their use of a larger basis set, however once the Davidson correction had been applied the result moved away from our results towards the experimental values. Finally the best theoretical results come from the second-order many-body perturbation theory of Ortiz (1998), who matches the experimental values excellently.

4.3. Resonances

Resonances were characterized using a Breit–Wigner fit to the eigenphase sums as implemented in the automated detection and fitting program RESON (Tennyson and Noble 1984). Eigenphase sums, which were obtained from diagonalizing

Table 2. CN^- bound states with energies given in eV. All calculations are for the equilibrium geometry of CN.

Model	Basis	Orbitals	Method	$^1\Sigma^+$ Binding energy
This work/1	cc-pVTZ	SCF	SE	2.594
2	cc-pVTZ	SCF	CC	3.485
3	aug-cc-pVTZ	SCF	SE	2.571
4	aug-cc-pVTZ	SCF	CC	3.820
5	aug-cc-pVTZ	NOs	CC	3.407
Thogersen and Olsen (2004)	cc-pVDZ		FCI	3.527
Midda and Das (2004)	aug-cc-pVTZ		HF/DF B3LYP	4.04
Polak and Fiser (2002)	aug-cc-pVQZ		CASSCF-MRCI	3.58
			w/Davidson	3.75
Ortiz (1998)	6-311++G(d,p)	UHF	2MBPT	3.83
Berkowitz *et al* (1969)			Experiment	3.82 ± 0.02
Klein *et al* (1983)			Experiment	3.821 ± 0.004
Bradforth *et al* (1993)			Experiment	3.86 ± 0.003

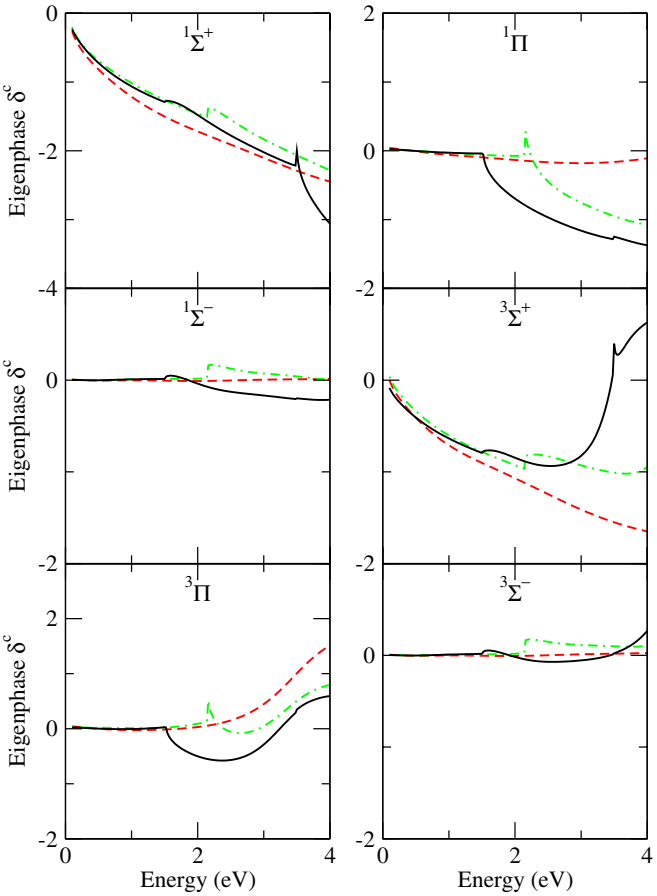

Figure 3. Electron–CN eigenphase sums for different symmetries for the SCF-SE (dash), SCF-CC (dash-dot) and NO-CC (solid) models.

the *K*-matrix for each symmetry at each energy, are displayed in figure 3. Only low-lying resonances were considered since higher resonances are unlikely to be important in any radiative association process.

A resonance manifests itself as a rapid increase by π radians in the eigenphase sum. This can best be seen in the $^3\Pi$ sum of the figure, where all three models undergo this change. Note we do not see the full shift of π as the widths of these resonances are large, spanning between 1–1.5 eV. The fitting of the Breit–Wigner form to a resonance can however be disrupted by the presence of threshold features in the eigenphase sum within the energy range of the fit. Threshold features are discontinuities in the eigenphase sum caused by the opening of new scattering channels. This can clearly be seen in both the $^1\Sigma^+$ and $^3\Sigma^+$ eigenphase sums of the NO-CC model, where the B $^2\Sigma^+$ excitation threshold of the target appears at 3.491 eV. The Breit–Wigner form explicitly does not allow for a partial resonance fit, thus when this occurs there is an uncertainty in the fitted data.

Table 3 summarizes the resonances detected for CN^-. The SE calculations both detect a single shape resonance of $^3\Pi$ symmetry at about 3.4 eV. At the SE level this is a very broad resonance with a width of about 1.5 eV. In the CC calculations this resonance position is systematically lowered, although for the cc-pVTZ basis set the width narrows and for the aug-cc-pVTZ basis it broadens. This is possibly because RESON had trouble finding this resonance in certain models (where thresholds were present), only a manual increase in the sensitivity of the programme allowed it to be fitted. Hence the widths do not appear consistent across similar models; the quoted values should probably be regarded as uncertain by up to 50%. The CC calculations based on the use of SCF orbitals introduce Feshbach resonances of $^3\Sigma^+$ and $^3\Sigma^-$ symmetry, with the use of an augmented basis set acting to raise the energy at which it appears by about 1 eV and 0.7 eV respectively. We note that none of these resonances lie below the A $^2\Pi$ first excited state of CN.

The quantum chemistry calculations on CN^- by Musial (2005), using the same aug-cc-pVTZ basis set as our final model, calculated excited states of the anion. These excited states would manifest in our scattering calculations as the sum in energies of an anionic bound state and a resonance (of the same symmetry). However the results in Musial (2005) are purely for singlet excited states, of which we have no resonances. This leads us to conclude that the excited states of CN^- detected by Musial (2005) are all false artefacts. The reasoning behind which can be found in the work of Stibbe and Tennyson (1999).

Interestingly we note that both HCN and HNC were found to support a single shape resonance of $^2\Pi$ symmetry at a position of between 2.5–3.3 eV and a width of between

Table 3. CN^- low-lying resonance positions (and widths) in eV.

Model	1	2	3	4	5
$^3\Sigma^+$		3.450 (0.761)		4.486 (0.462)	4.526 (1.186)
$^3\Pi$	3.359 (1.513)	2.978 (1.053)	3.424 (1.403)	3.340 (1.583)	3.208 (1.084)
$^3\Sigma^-$		4.613 (1.209)		5.319 (0.906)	4.881 (1.084)

Table 4. X $^2\Sigma^+$ target energies, A $^2\Pi$ & B $^2\Sigma^+$ excitation energies, and $^1\Sigma^+$ bound state energies for different bond lengths, All values are in eV.

Bond length (Å)	X $^2\Sigma^+$	A $^2\Pi$	B $^2\Sigma^+$	$^1\Sigma^+$ Binding energy
0.9718	−92.252	3.092	3.212	3.178
1.0718	−92.354	2.206	3.341	3.326
1.1718 (equilibrium)	−92.381	1.515	3.491	3.407
1.2718	−92.371	1.014	3.651	3.414
1.3718	−92.338	0.589	3.622	3.411

1.3–1.6 eV depending on the model used (Varambhia and Tennyson 2007).

5. Results as a function of bond length

As a further development to our calculations we ran the same model (aug-cc-pVTZ basis set, NO-CC scattering model) at different bond lengths, spanning 0.5 Å and centred on the equilibrium geometry of 1.1718 Å. Table 4 presents the results of the target calculation as a function of bond length and also the binding energy of the anionic bound state detected in the scattering calculation.

Table 5 gives resonance positions for the $^3\Sigma^+$, $^3\Pi$ and $^3\Sigma^-$ resonances as a function of bond length. As bond length increases we find that all resonances lower in position and narrow in their widths. At the smallest bond length we were unable to fit the width of the $^3\Pi$ resonance. This is due to the extreme broadness the resonance is likely to have, resulting in it crossing over threshold features which RESON is unable to make a fit of. Our calculations also detected a $^3\Delta$ state at 1.2718 and 1.3718 Å, at 1.2718 Å it lies very close to the $^3\Sigma^-$; thus we were unable to obtain a position fit for this resonance despite its clear appearance in the eigenphase sums. The value of 4.1 eV given in table 5 is a result of a manual fit, whereby we have taken the second derivative of the eigenphase sum to find the position of the point of inflection. The $^3\Delta$ resonance is observable in the eigenphase sums at all bond lengths, however due to its proximity to $^3\Sigma^-$ and the increased broadness of all resonances at lower bond lengths, we were not able to obtain RESON fits for this $^3\Delta$ resonance.

6. Conclusions

In this work we have presented excitation cross-sections to the first two excited states of CN which represent the 'CN red' and 'CN violet' spectral lines. Applying the Born correction to these cross-sections leads to an enhancement of the magnitude of both. It must also be considered that this enhancement is already pronounced at the maximum incident electron energy in our calculations. At 10 eV the size of the cross-section has approximately doubled due to the correction. A typical plasma may contain electrons moving at much greater energies than 10 eV; thus if we were to extend our results up to and beyond ionization of the molecule (into the high-energy scattering regime), this enhancement will be even more pronounced. This is because at these energies the Born approximation becomes dominant. This increase in cross-section magnitude will lead to an increase in the reaction rates calculated for these excitations, likely leading to an enhancement of the spectra modelled from this data.

Thus far the role of electron-scattering cross-sections in the interstellar medium (ISM) has largely been ignored, in preference to the use of reaction rates. Due to this there is no data with which to compare our excitation cross-sections to, and to our knowledge we believe our data to be the first low-energy electronic excitation cross-sections for this molecule. Comparisons with plasma models are also difficult, as these all assume non-local thermal equilibrium. Because of this the plasma spectra can be predicted from these models, however reaction rates cannot. Thus no direct comparisons with existing plasma data can be made.

Our calculations have also given data which suggest there are no scattering resonance features at low energy, below 3 eV. This makes it unlikely that the formation on CN^- in the ISM is caused by the trapping of an incoming electron into a resonance state of neutral molecule. The temperatures in the ISM are simply too low to produce electrons with enough energy to become trapped in one of these states.

As discussed in Harrison and Tennyson (2011), an alternative explanation of the observed molecular anion abundance may arise from the very weakly bound anionic states. These states will support nuclear excited states which lie in the continuum and therefore are resonances. However, it appears that CN^- does not support any of these states

Table 5. Resonance position (and widths) in eV as a function of bond length. *a* indicates a manual fit.

Bond length (Å)	0.9718	1.0718	1.1718 (equilibrium)	1.2718	1.3718
$^3\Sigma^+$	7.55 (2.01)	5.71 (1.35)	4.526 (1.186)	2.08 (0.25)	1.03 (0.08)
$^3\Pi$	9.72(*a*)	7.76 (3.14)	3.208 (1.084)	2.64 (0.84)	2.08 (0.52)
$^3\Sigma^-$	9.04 (2.89)	6.64 (1.73)	4.881 (1.084)	4.1*a*	2.40 (0.43)

either. It would therefore seem likely that the vast majority interstellar CN^- is formed by some other mechanism, such as by dissociative attachment of a CN containing species.

An important electron collision process not considered here is electron impact rotation excitation. In an extension to this work, we are developing the theory for calculating spin-coupled rotationally excited cross-sections, and from this rotational excitation calculations on CN^-. The results of these calculations will be reported elsewhere.

Acknowledgments

The first author would like to thank R Harrison and E Brunetti for their support and STFC for a studentship.

References

Agundez M *et al* 2010 *Astron. Astrophys. Lett.* **517** L2
Ajitha D and Hirao K 2001 *Chem. Phys. Lett.* **347** 121–6
Baluja K L, Mason N J, Morgan L A and Tennyson J 2000 *J. Phys. B: At. Mol. Opt. Phys.* **33** L677–84
Berente I, Szalay P G and Gauss J 2002 *J. Chem. Phys.* **117** 7872–81
Berkowitz J, Chupka W A and Walter T A 1969 *J. Chem. Phys.* **50** 1497–500
Bradforth S E, Kim E H, Arnold D W and Neumark D M 1993 *J. Chem. Phys.* **15** 800–10
Brunger M J and Buckman S J 2002 *Phys. Rep.* **357** 215–458
Burke P G 2011 *R-Matrix Theory of Atomic Collisions: Application to Atomic, Molecular and Optical Processes* (Berlin: Springer)
Faure A, Gorfinkiel J D, Morgan L A and Tennyson J 2002 *Comput. Phys. Commun.* **144** 224–41
Gottlieb C A, Brunken S, McCarthy M C and Thaddeus P 2007 *J. Chem. Phys.* **126** 191101
Halpern J B, Huang Y and Titarchuk T 1996 *Astrophys. Space Sci.* **236** 11–7
Harrison S and Tennyson J 2011 *J. Phys. B: At. Mol. Opt. Phys.* **44** 045206
Herbst E and Osamura Y 2008 *Astrophys. J.* **679** 1670–9
Huber K P and Herzberg G 1997 *NIST Chemistry WebBook, NIST Standard Reference Database Number 69* ed P J Linstrom and W G Mallard (Gaithersburg, MD: National Institute of Standards and Technology) p 20899 http://webbook.nist.gov
Joshipura K N and Patel P M 1994 *Z. Phys.* D **29** 269–73
Kalcher J 2002 *Phys. Chem. Chem. Phys.* **4** 3311–7
Klein R, McGinnis R P and Leone S R 1983 *Chem. Phys. Lett.* **100** 475–8
Leach S 2012 *Mon. Not. R. Astron. Soc.* at press
Liu Y, Duan C, Lie H, Guo H, Guo Y, Liu X and Lin J 2001 *J. Mol. Spectrosc.* **205** 16–9
Midda S and Das A K 2004 *Int. J. Quantum Chem.* **98** 447–55
Morgan L A, Tennyson J and Gillan C J 1998 *Comput. Phys. Commun.* **114** 120–8
Musial M 2005 *Mol. Phys.* **103** 2055–60
Ortiz J V 1998 *Chem. Phys. Lett.* **296** 494–8
Polak R and Fiser J 2002 *J. Mol. Struct.* **584** 69–77
Sarpal B K, Branchett S E, Tennyson J and Morgan L A 1991 *J. Phys. B: At. Mol. Opt. Phys.* **24** 3685–99
Shi D, Li W, Sun J and Zhu Z 2011 *J. Quant. Spectrosc. Radiat. Transfer* **112** 2335–46
Sordo J A 2001 *J. Chem. Phys.* **114** 1974–80
Stibbe D T and Tennyson J 1999 *Chem. Phys. Lett.* **308** 532–6
Tennyson J 2010 *Phys. Rep.* **491** 29–76
Tennyson J, Brown D B, Munro J J, Rozum I, Varambhia H N and Vinci N 2007 *J. Phys. Conf. Ser.* **86** 012001
Tennyson J and Noble C J 1984 *Comput. Phys. Commun.* **33** 421–4
Thaddeus P 1972 *Annu. Rev. Astron. Astrophys.* **10** 305–34
Thogersen L and Olsen J 2004 *Chem. Phys. Lett.* **393** 36–43
Thompson R and Dalby F W 1968 *Can. J. Phys.* **46** 2815–9
Varambhia H N and Tennyson J 2007 *J. Phys. B: At. Mol. Opt. Phys.* **40** 1211–33
Werner H J *et al* 2008 Molpro, version 2008.3, a package of *ab initio* programs see http://www.molpro.net